Chinese Chemical Letters 35 (2024) 109365

Contents lists available at ScienceDirect

Chinese Chemical Letters

journal homepage: www.elsevier.com/locate/cclet

Near-infrared organic lasers with ultra-broad emission bands by simultaneously harnessing four-level and six-level systems

Lei Wang[a], Jun-Jie Wu[a], Chang-Cun Yan[b,*], Wan-Ying Yang[a], Zong-Lu Che[a], Xin-Yu Xia[a], Xue-Dong Wang[a,**], Liang-Sheng Liao[a,c,**]

[a] Jiangsu Key Laboratory for Carbon-Based Functional Materials & Devices, Institute of Functional Nano & Soft Materials (FUNSOM), Soochow University, Suzhou 215123, China
[b] Jiangsu Engineering Laboratory of Novel Functional Polymeric Materials, College of Chemistry, Chemical Engineering and Materials Science, Soochow University, Suzhou 215123, China
[c] Macao Institute of Materials Science and Engineering, Macau University of Science and Technology, Macau SAR 999078, China

ARTICLE INFO

Article history:
Received 26 September 2023
Revised 24 November 2023
Accepted 3 December 2023
Available online 5 December 2023

Keywords:
Excited-state intramolecular proton transfer
Organic solid-state laser
Wide gain interval
Near-infrared emission
Molecular design

ABSTRACT

Organic lasers with broad emission bands in near-infrared (NIR) region are crucial for their applications in laser communication, night-vision as well as bioimaging owing to the abundance of selectable lasing wavelengths. However, for most organic gain materials, gain regions are limited in a small wavelength range because of the fixed energy level systems. Herein, we design a strategy to realize NIR organic lasers with broad emission bands based on tunable energy level systems induced by cascaded excited-state intramolecular proton transfer (ESIPT). A novel gain material named DHNN was developed, which can undergo a cascaded double-ESIPT process supporting four-level and six-level systems simultaneously. By doping DHNN into polystyrene microspheres, NIR lasers with tunable emission bands can be achieved based on the careful modulation of microcavities. Finally, organic lasers with an ultra-broad emission band ranging from 700 nm to 900 nm was successfully achieved by harnessing four-level and six-level systems simultaneously.

© 2024 Published by Elsevier B.V. on behalf of Chinese Chemical Society and Institute of Materia Medica, Chinese Academy of Medical Sciences.

Since solid-state lasers (SSLs) initially suggested in 1960, they have developed quite quickly [1]. Organic SSLs (OSSLs) have been recognized as a promising alternative to conventional lasers due to their numerous advantages including compact and durable structure [2], affordability [3], various active medium [4], and a relatively simple fabrication process. Near-infrared (NIR) lasers (780–2526 nm) hold significant promise in various fields such as laser communication, spectroscopy, night vision, and more, making them a compelling choice for numerous applications, with excellent tissue penetration and low waveguide loss, have drawn a lot of attention [5–7]. In recent years organic solid-state lasers have also been combined with OLEDs to develop indirect electroluminescent organic solid-state lasers. Nevertheless, most NIR OSSLs proposed so far can only lase in a very narrow wavelength range because of the fixed energy level systems [8–12]. In this case, at least two or three different lasers should be adopted in attempting to change the emission wavelength in abroad wavelength region, which result in ahigh cost and device complexity. Therefore, NIR OSSL with a broad emission band is in high urgent need.

In most OSSLs, stimulated emission can only occur between specific energy levels, in which population inversion can be effectively constructed. For most organic gain materials, laser emission can only be achieved at 0–1 peak built upon *quasi*-four-level systems, resulting in a narrow emission band (Fig. 1, left part). In ESIPT-active organic gain materials, it is possible to create a real four-level system that not only lowers the lasing threshold but also redshifts the emission band [13–19]. More importantly, compared with the emission band in normal form, a new emission band can be realized in tautomer form [20–24]. Therefore, constructing multi-energy level systems can be an effective means of regulating the emission band of OSSLs. However, the resulting emission band is still very narrow, because stimulated emission can only occur in tautomer form with easier population inversion (Fig. 1, right part). Recently, by harnessing a cascaded double ESIPT process, we achieved a six-level system lasing beyond 850 nm [10]. Although there are two tautomer forms in the six-level system, stimulated

* Corresponding author.
** Corresponding authors at: Jiangsu Key Laboratory for Carbon-Based Functional Materials & Devices, Institute of Functional Nano & Soft Materials (FUNSOM), Soochow University, Suzhou 215123, China.
E-mail addresses: cyan@suda.edu.cn (C.-C. Yan), wangxuedong@suda.edu.cn (X.-D. Wang), lsliao@suda.edu.cn (L.-S. Liao).

https://doi.org/10.1016/j.cclet.2023.109365
1001-8417/© 2024 Published by Elsevier B.V. on behalf of Chinese Chemical Society and Institute of Materia Medica, Chinese Academy of Medical Sciences.

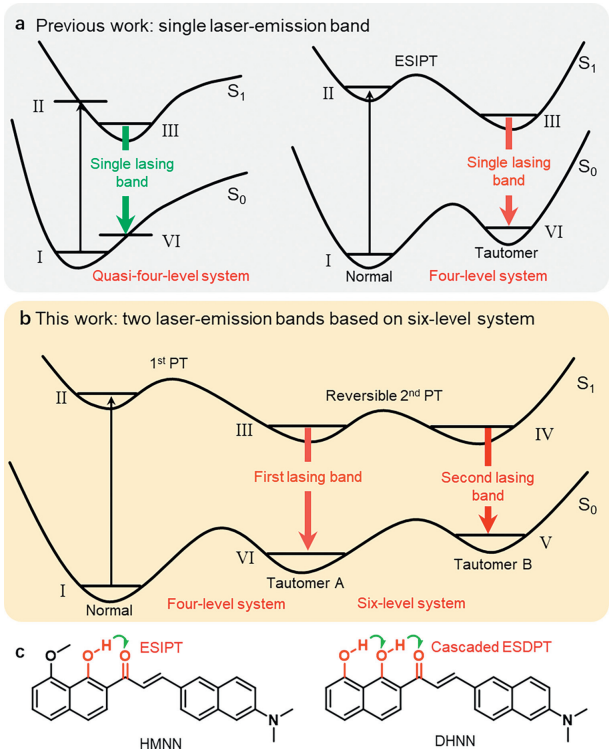

Fig. 1. (a) The sketch of single laser emission band based on *quasi*-four- and four-level systems. (b) The sketch of two laser emission bands on six-level system. (c) Chemical structures of HMNN and DHNN: proton transfer sites are labelled by green arrows.

emission can only be achieved in the last tautomer form leading to a narrow emission band [25,26]. In our recent work, the emission wavelength was further red-shifted by carefully designing the ESIPT parent core [11]. It is worth noting that a four-level system laser can also be established in such a system through a meticulous molecular design. We have been inspired by this work to propose the possibility of four-level laser generation and the simultaneous existence of six-level lasers. Consequently, the combination of these two distinct emission bands may lead to the generation of a broad emission spectrum (Fig. 1b).

Herein, based on above considerations, we developed an novel ESIPT-active organic matter (*E*)−1-(1,8-dihydroxynaphthalen-2-yl)−3-(6-(dimethylamino)naphthalen-2-yl)prop−2-en-1-one (DHNN) featured with two adjacent intramolecular hydrogen bonds. When doped in polystyrene (PS) microspheres, laser emission based on ESIPT four- and six-energy systems can be achieved, and the laser emission bands can be tuned form narrow to wide by changing the size of the resonators. Moreover, HMNN and DMNN were also synthesized by respectively introducing one and two methyl groups in DHNN to eliminate the proton transfer site. Further comparison shows that the molecule DHNN can be used as a gain medium to achieve a wide wavelength range of laser emission. This organic solid-state laser enables selectable laser emission over a long wavelength range from deep red to near-infrared in a single laser device, which can be further applied in wavelength-tunable NIR organic lasers in theory.

In order to enable the generation of four-level lasers and the simultaneous existence of six-level lasers in a gain medium, we firstly designed DHNN with a 6-dimethylamono-2-naphthyl group as electron donor for our studies. The naphthyl group can also expand the conjugated system and thus tune the energy levels of excited states. In addition, HMNN, which allows only one possible ESIPT process, was designed as a control compound. DHNN and HMNN were synthesized from commercially available 1,8-naphthalenediol through a five-step method (Scheme 1). At first, after the protection of hydroxyl groups, compound **2** can be converted into compound **4** by a two-step acetylation reaction. Then, DMNN can be obtained as a key intermediate compound through the Claisen–Schmidt reaction of compound **4** and 6-dimethylamino-2-naphthaldhyde. As a fully methylated compound of DHNN, DMNN can be used as a control compound to study the optoelectronic properties before ESIPT process. Finally, DHNN was be obtained by a demethylation reaction with boron tribromide, and DMNN was obtained by a selective demethylation with boron trichloride. Every compound underwent characterization through analysis of ^{1}H NMR spectra and ^{13}C NMR spectra (Figs. S1–S8 in Supporting information).

As shown in Fig. 2a, a two-step cascaded ESIPT process in DHNN was proposed according to our previously reported work. Following the initial proton transfer step, tautomer A (TA) can be produced, and subsequently, tautomer B (TB) can be generated through the second proton transfer process. To prove this stepwise ESIPT process, density functional theory (DFT) calculations were performed at first. Fig. 2b illustrates the calculated energies of the S_0 and the S_1 for the normal form (N), tautomer A (TA), tautomer B (TB), and their corresponding transition states. The proton transfer from N* to TA* was calculated to be barrierless, indicating the spontaneous process. But on the contrary, TA* has a lower relative energy than TB* by 11.7 kcal/mol. Additionally, we can see that the relative energy of TB* is lower than N* by about 9.4 kcal/mol. It means that TA* is more stable than TB* in thermodynamics and thus the proton transfer form TA* to TB* is quite difficult. After carefully optimization, a transition state can be obtained between TA* and TB*, and the relative energy of TS* is 1.4 kcal/mol lower than TB* and 10.3 kcal/mol higher than TA*. Although the energy barrier is a little higher than that can be crossed spontaneously, the proton transfer can still proceed under thermal activation at room temperature [27]. In S_0, all ground state proton transfer processes were calculated to be barrierless. From above analyses, the four-level system in DHNN is proved to be preferred and the six-level system is also possible.

Next, the UV–vis absorption and PL spectroscopy were performed on HMNN and DHNN, respectively. As shown in Fig. S10 (Supporting information), both of absorption and PL of DHNN and HMNN exhibited dramatically redshift when increasing to polarity of solvents, indicating the intramolecular charge transfer interactions in these two materials. Comparing PL spectra of DHNN with HMNN in dichloromethane, the main PL peak of DHNN is a little redshift maybe because of the extended absorption. More interestingly, there is a new PL peak around 760 nm for DHNN which is absent in PL spectrum of HMNN. This new peak can be attributed to the emission of TB*, since the ESIPT proceeds more easily in solvents with a higher polarity [28]. To further study the optoelectronic properties of our well-designed materials, the absorption and PL spectra were acquired by doping them into PS films. As displayed in Fig. 3a, the absorption and PL of HMNN showed dramatically redshift compared with that of DMNN, which is induced by the ESIPT process in HMNN. For DHNN, the absorption and PL further red-shifted on the basis of HMNN. Considering that there is only one ESIPT can proceed at maximum in HMNN according to the inherent limitations imposed by proton transition sites, the redshift of the PL of DHNN may be assigned to TB* emission.

Evidences can be found in time-resolved fluorescence spectra. Fig. S11 (Supporting information) showed that there is only one Excited state in DMNN since the lifetimes of DMNN at 420 nm, 540 nm and 640 nm are calculated to be same ($\tau = 2.2$ ns). When we test the lifetime of HMNN, the data at 640 nm and 750 nm are almost same (Fig. 3b), too. Differently, two lifetimes can be obtained at each wavelength indicating two transition channels. The

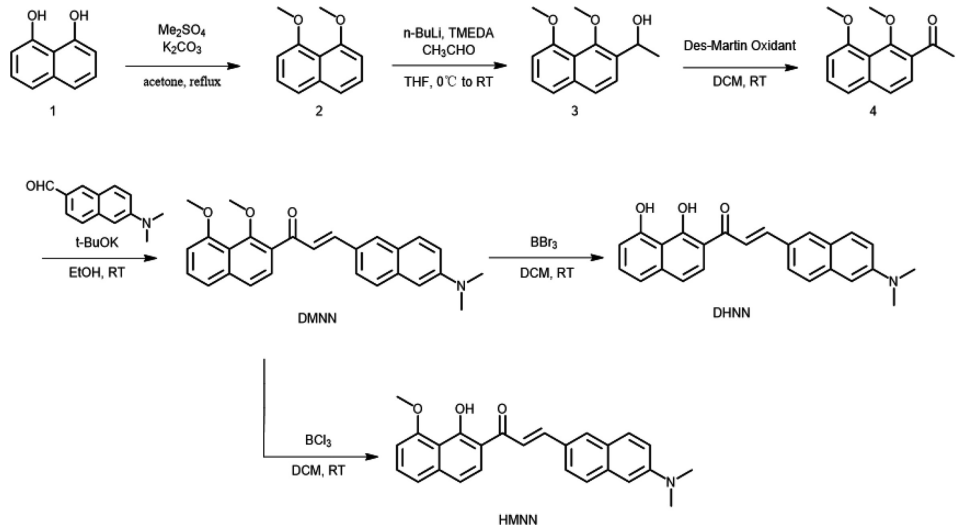

Scheme 1. Synthetic route of DMNN, DHNN and HMNN.

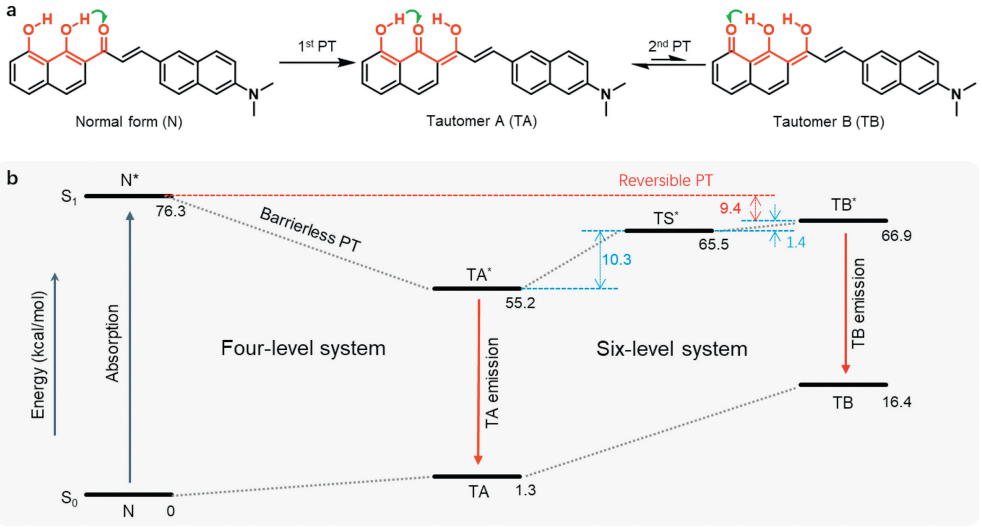

Fig. 2. (a) Schematic process of two step-by-step proton transfers in the molecule DHNN. (b) The calculated relative energy levels of DHNN during the ESIPT.

shorter lifetimes were less than 1 ns which may be relation to the ESIPT process according to previous reports [10,29]. For DHNN, the lifetimes at 700 nm, 750 nm (the wavelength at maximum) and 850 nm were calculated respectively. The results are displayed in Figs. 3c–e. Similar lifetimes can be obtained at 700 nm ($\tau_1 = 0.7$ ns, $\tau_2 = 5.5$ ns) and 750 nm ($\tau_1 = 0.7$ ns, $\tau_2 = 5.8$ ns), showing the same excited state. However, different lifetimes at 850 nm ($\tau_1 = 0.6$ ns, $\tau_2 = 8.9$ ns) were obtained, displaying that the PL at 850 nm may originate from a different excited state. Combined with above analyses, we can conclude that the PL at 850 nm of DHNN should be contributed by TB* emission. Therefore, the cascaded double ESIPT process can be proved to proceed in PS film at room temperature. It should be noted that the PL of DHNN mainly comes from TA* emission, which is accordance to the results of DFT calculations.

For the study of the properties of laser, microspheres are made by doping target molecules into PS in a certain ratio [30]. Initially, to ascertain the level of doping, PS films doped with HMNN and DHNN with varied doping agent concentrations ranging from 0.1% to 2.0% were prepared. Based on the UV–vis absorption and PL spectra displayed in Figs. S12–S15 (Supporting information), the absorption and PL properties are almost same in different doping concentration for both of HMNN and DHNN. Thus, 1.0% was chosen as the doping concentration in the preparation of PS microspheres. Next, based on previously reported work, a microemulsion method (Fig. S16 in Supporting information) was employed and PS microspheres doped with DMNN, HMNN and DHNN were successfully fabricated [31]. As demonstrated in Fig. S17 (Supporting information), the resulting PS microspheres exhibited uniform morphologies and smooth surfaces. These characters of the well-prepared microspheres endowed them with the ability to confine photons by continuous total internal reflection, forming whispering gallery mode (WGM) resonators. Therefore, WGM laser devices were successfully fabricated.

Subsequently, using a previously described technique, laser performances of the selected microspheres were tested (Fig. S18 in Supporting information). As shown in Fig. 4a, the target molecule HMNN was doped with PS to create microspheres with a diameter (D) of 5.6 μm, which were used for laser testing. When pumped with a 532-nm pulse laser, we can observe laser emission and its central wavelength is about 710 nm. From Fig. 4b, the threshold was calculated as 13.6 μJ/cm^2. For a DHNN-doped microsphere (inset in Fig. 4c), laser emission was proved to occur around 770 nm (Fig. 4a). From Fig. 4b, it is easy to see the threshold is 27.61 μJ/cm^2 at which the microspheres produce laser light. Although

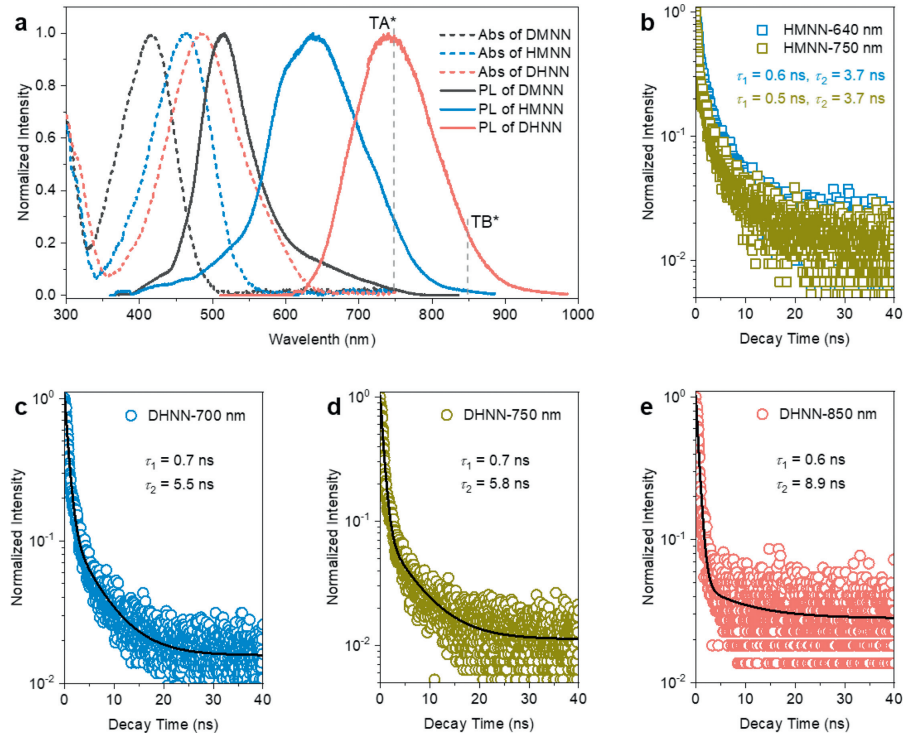

Fig. 3. (a) For a film mixture containing DMNN, HMNN, and DHNN, the photoluminescence and UV–vis absorption spectra were obtained. The approximate peak positions of TA * and TB *. Fluorescence decay of HMNN-doped PS films measured at 640 nm and 720 nm (b), 700 nm ($\tau_1 = 0.7$ ns, $\tau_2 = 5.5$ ns) (c), 750 nm ($\tau_1 = 0.7$ ns, $\tau_2 = 5.8$ ns) (d) and 850 nm ($\tau_1 = 0.6$ ns, $\tau_2 = 8.9$ ns). (e) The DHNN fluorescence of the PS films began to deteriorate.

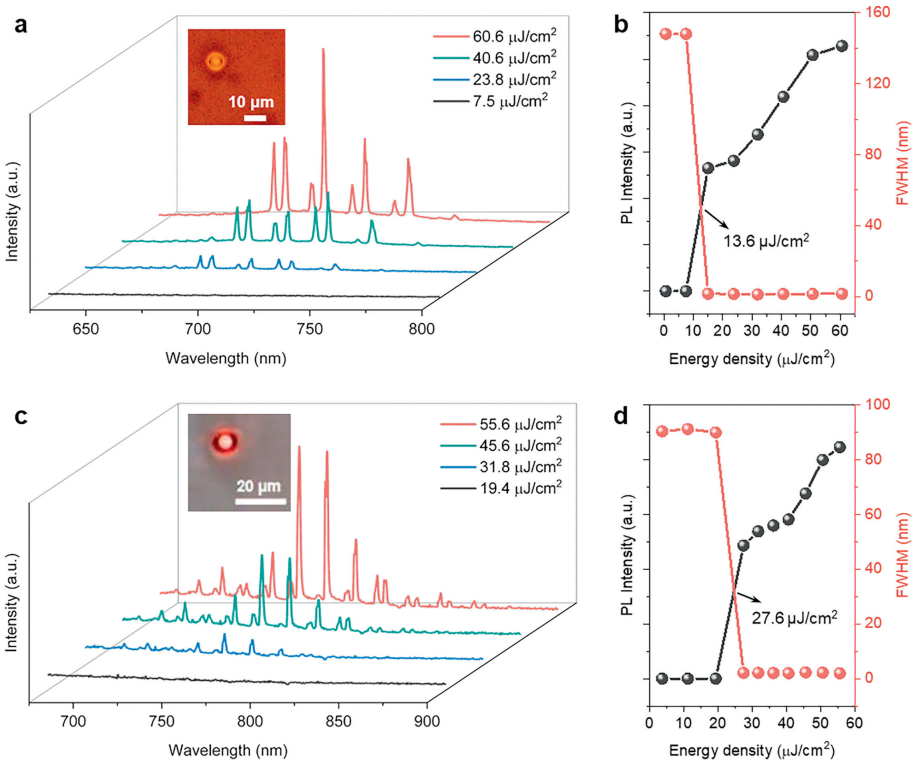

Fig. 4. (a) PL spectra recorded with 5.6 μm diameter HMNN PS microspheres excited at different energies. Left inset: bright-field optical micrograph of the selected HMNN-doped PS microsphere. (c) PL spectra recorded with 11.1 μm diameter DHNN PS microspheres excited at different energies. Left inset: bright-field optical micrograph of the selected DHNN-doped PS microsphere. Profiles of power-dependent photoluminescence (PL) intensities (represented by black spheres) and FWHM (represented by red spheres) are presented depending on the optical pump density. (b) HMNN doped PS microsphere. (d) DHNN doped PS microsphere.

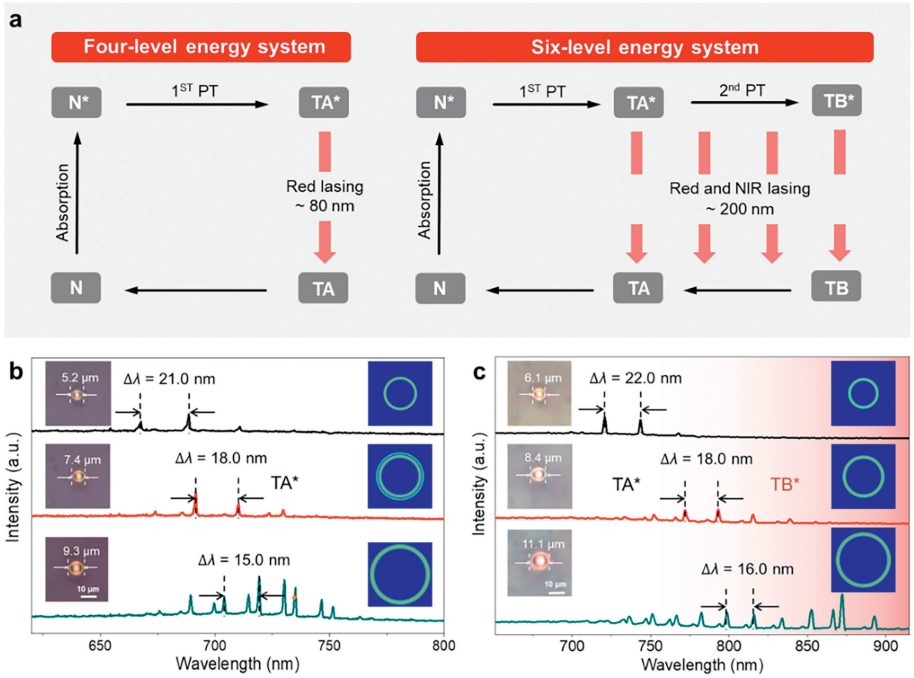

Fig. 5. (a) Schematic illustration of the laser emission of HMNN based on four-level system and the proposed laser emission of DHNN based on four-level and six-level systems simultaneously. (b) The laser spectra of three HMNN-doped microspheres with the sizes of 5.2, 7.4, and 9.3 μm in diameter. (c) The laser spectra of three DHNN-doped microspheres with the sizes of 6.1, 8.4, and 11.1 μm in diameter. Left insets in (c) and (d): bright-field optical micrographs of the chosen DHNN-doped PS microspheres. Right inset in (c) and (d): simulated distribution of electromagnetic fields in microspheres with different sizes. The color indicates the field density increasing from blue to red.

there is a 60-nm redshift compared with HMNN, the laser emission of DHNN is still in the range of TA* emission according to the PL spectra in Fig. 3a. The events showed that, the four-level system lasing is preferred within DHNN although a six-level system can also be formed. It indicated that, the real four-level system is crucial for the realization of laser emission in our prepared materials. Finally, the stability test showed that both of the lasers based on HMNN and DHNN showed good stability in 5000 pumping shots (Figs. S19 and S20 in Supporting information). And the organic molecule DMNN, which was used for comparison, was also prepared into PS spheres by us using the above method for laser testing, and it was finally found that there was indeed no laser signal generation as we initially suspected (Fig. S21 in Supporting information). From the experimental results we can clearly see that the molecule DMNN is not able to generate laser light in the WGM resonance cavity by optical pumping and thus particle number inversion compared to the two organic molecules in the main text.

Although NIR laser emission can be achieve by HMNN, the emission band was still very narrow and only a four-level system lasing can be realized. As shown in Fig. 5a, for HMNN only a four system can be formed resulting a red lasing with emission band about 80 nm. However, for DHNN, a six-level system can also exist. If six-level system lasing is able to be established simultaneously, the laser emission band can be dramatically broadened. As the resonator engineering is an effective method to tune laser emission in tunable lasers, we start to investigate the laser performance of microspheres with different sizes [24]. The size of PS microspheres can be easily tuned based on previously reported work. We can clearly observe that the laser produced a certain redshift with increasing the sphere diameters. It is noteworthy that for HMNN-doped microspheres, with the increase of the diameter, the central wavelength can reach 760 nm (Fig. 5b). But the laser wavelength can not be further extended because of the limitation of the gain region based on the four-level system. On the contrary, for DHNN-doped microspheres, with the increase of the diameter a new laser emission band can be observed with the central wavelength around 870 nm (Fig. 5c). And thus, an ultra-broad emission band can be achieved reaching about 200 nm. According to the above analyses, the new lasing band should be derived from TB emission.

To add to the above changes caused by changing the modulus of the microspheres, we have done the following. Figs. S22 and S23 (Supporting information) show the plots of the mode spacing $\Delta\lambda_m$ *versus* 1/D of HMNN and DHNN microspheres, demonstrating clearly linear relationships, which matched well with the following formula.

$$\Delta\lambda_m = \frac{\lambda^2}{L\left[n - \lambda\left(\frac{d_n}{d\lambda}\right)\right]} \quad (1)$$

The results proved that the lasers were achieved based on WGM resonators. We aim to highlight the excellent light limiting characteristics in the self-made microsphere WGM resonant cavity, the electric field stitching inside the microspheres of different sizes was simulated, which can also prove the laser emission in WGM (the right insets of Figs. 5b and c). Therefore, we successfully achieved four-level system laser and six-level system laser using only one gain material through resonator engineering.

In summary, an organic molecule DHNN which is distinguished by two adjacent intramolecular hydrogen bonds serving as the building block of the cascaded ESIPT process was designed and synthesized. The cascaded ESIPT process was proved to be able to proceed in DHNN using spectroscopic analyses and theoretical calculations. It showed that laser emissions from both TA*-TA and TB*-TB at the same time are possible. Additionally, laser emissions were made based on a four-level and six-level energy system under stimulation by doping the molecule into PS microspheres. Importantly, DHNN allows for selective laser emission in a single solid-state laser over a wide wavelength range, from deep red to near-infrared. In conclusion, we have successfully developed an

NIR organic laser with an ultra-broad emission band by harnessing four-level and six-level systems simultaneously, which will greatly facilitate the development of organic lasers in practice in the near future.

Declaration of competing interest

The authors declare that they have no known competing financial interests or personal relationships that could have appeared to influence the work reported in this paper.

Acknowledgments

The authors acknowledge the financial support from the National Natural Science Foundation of China (Nos. 21971185, 52173177, 22105139), the Natural Science Foundation of Jiangsu Province (Nos. BK20230010, BK20221362), and the Science and Technology Support Program of Jiangsu Province (No. TJ-2022-002). This project is funded by Jiangsu Key Laboratory for Carbon-Based Functional Materials & Devices, Soochow University (No. KJS2156), Collaborative Innovation Center of Suzhou Nano Science & Technology (CIC-Nano), the "111" Project, Joint International Research Laboratory of Carbon-Based Functional Materials and Devices, and Soochow University Tang Scholar.

The authors would like to thank Chang Wang from Shiyanjia Lab (www.shiyanjia.com) for the help of DFT calculation.

Supplementary materials

Supplementary material associated with this article can be found, in the online version, at doi:10.1016/j.cclet.2023.109365.

References

[1] T.H. Maiman, Nature 187 (1960) 493–494.
[2] M.D. McGehee, A.J. Heeger, Adv. Mater. 12 (2000) 1655–1668.
[3] S. Singh, V.R. Kanetkar, G. Sridhar, V. Muthuswamy, K. Raja, J. Lumin. 101 (2003) 285–291.
[4] I.D.W. Samuel, G.A. Turnbull, Chem. Rev. 107 (2007) 1272–1295.
[5] C. Grivas, M. Pollnau, Laser Photonics Rev. 6 (2012) 419–462.
[6] M.T. Hill, M.C. Gather, Nat. Photonics 8 (2014) 908–918.
[7] R.M. Ma, R.F. Oulton, Nat. Nanotechnol. 14 (2019) 12–22.
[8] J.J. Wu, H.F. Gao, R. Lai, et al., Matter 2 (2020) 1233–1243.
[9] C.C. Yan, X.D. Wang, L.S. Liao, ACS Photonics 7 (2020) 1355–1366.
[10] J.J. Wu, M.P. Zhuo, R. Lai, et al., Angew. Chem. Int. Ed. 60 (2021) 9114–9119.
[11] C.C. Yan, Y.P. Liu, W.Y. Yang, et al., Angew. Chem. Int. Ed. 61 (2022) e202210422.
[12] W.Y. Yang, R.C. Lai, J.J. Wu, et al., Adv. Funct. Mater. 32 (2022) 2204129.
[13] T. Mutai, H. Tomoda, T. Ohkawa, Y. Yabe, K. Araki, Angew. Chem. Int. Ed. 47 (2008) 9522–9524.
[14] P.W. Zhou, K. Han, Acc. Chem. Res. 51 (2018) 1681–1690.
[15] C.C. Yan, J.J. Wu, W.Y. Yang, et al., Sci. China Mater. 65 (2022) 1020–1027.
[16] Z.L. Che, C.C. Yan, X.D. Wang, L.S. Liao, Chin. J. Chem. 40 (2022) 2468–2481.
[17] W.Y. Yang, C.C. Yan, X.D. Wang, L.S. Liao, Sci. China Chem. 65 (2022) 1843–1853.
[18] J.J. Wu, X.D. Wang, L.S. Liao, Laser Photonics Rev. 16 (2022) 2200366.
[19] J.J. Wu, S.W. Yu, Y.P. Liu, et al., Adv. Funct. Mater. 33 (2023) 2214308.
[20] A.U. Khan, M. Kasha, Proc. Natl. Acad. Sci. 80 (1983) 1767.
[21] X. Cheng, K. Wang, S. Huang, et al., Angew. Chem. Int. Ed. 54 (2015) 8369–8373.
[22] W. Zhang, Y.L. Yan, J.M. Gu, J.N. Yao, Y.S. Zhao, Angew. Chem. Int. Ed. 54 (2015) 7125–7129.
[23] X. Cheng, Y.F. Zhang, S.H. Han, et al., Chem. Eur. J. 22 (2016) 4899–4903.
[24] X.D. Wang, Q. Liao, H. Li, et al., J. Am. Chem. Soc. 137 (2015) 9289–9295.
[25] G.Q. Wei, Y. Yu, M.P. Zhuo, X.D. Wang, L.S. Liao, J. Mater. Chem. C 8 (2020) 11916–11921.
[26] C.Y. Peng, J.Y. Shen, Y.T. Chen, et al., J. Am. Chem. Soc. 137 (2015) 14349–14357.
[27] H.W. Tseng, J.Q. Liu, Y.A. Chen, et al., J. Phys. Chem. Lett. 6 (2015) 1477–1486.
[28] A.P. Demchenko, K.C. Tang, P.T. Chou, Chem. Soc. Rev. 42 (2013) 1379–1408.
[29] C.C. Yan, Z.L. Che, W.Y. Yang, X.D. Wang, L.S. Liao, Opo-Electron. Adv. 6 (2023) 230007.
[30] Y.X. Du, C.L. Zou, C.H. Zhang, et al., Light Sci. Appl. 9 (2020) 151.
[31] C. Wei, S.Y. Liu, C.L. Zou, et al., J. Am. Chem. Soc. 137 (2015) 62–65.